ELSEVIER

Non-linear feature identifications based on self-sensing impedance measurements for structural health assessment

Amanda C. Rutherford, Gyuhae Park[*], Charles R. Farrar

Los Alamos National Laboratory, Engineering Sciences & Applications, The Engineering Institute, Mail Stop T001, Weapon Response Group, Los Alamos, NM 87545, USA

Abstract

This paper presents the application of a non-linear feature identification technique for structural damage detection. This method is coupled with the impedance-based structural health monitoring (SHM) method, which utilises electro-mechanical coupling properties of piezoelectric materials. The non-linear feature examined in this study is in the form of autoregressive coefficients in the frequency domain autoregressive model with exogenous (ARX) inputs, which explicitly considers non-linear system input/output relationships. The applicability of this non-linear feature for damage identification is investigated in various frequency ranges using impedance signals measured from a laboratory-test structure. The performance of the non-linear feature is also compared with those of linear features typically used in impedance methods. This paper reinforces the utility of non-linear features in SHM and suggests that their sensitivity in different frequency ranges may be leveraged for certain applications.
Published by Elsevier Ltd.

Keywords: Structural health monitoring; Nonlinearity; Active-sensing; Impedance-based structural health monitoring

1. Introduction

The process of implementing a damage detection strategy for aerospace, civil, and mechanical infrastructures is referred to as structural health monitoring (SHM). Damage here is defined as changes to the material and/or geometric properties of these systems, which adversely affects the current or future performance of the systems. The SHM process involves the observation of a system over time using periodically spaced dynamic response measurements, the extraction of damage sensitive features from these measurements, and the statistical analysis of these features to determine the current state of system health.

Recently, the structural community has turned its attention to developing high-frequency, in-service damage identification techniques that provide required sensitivity to localised, minor defects in a system. Piezoelectric (PZT) materials are particularly useful for this purpose because they can perform both duties of sensing and

*Corresponding author. Tel.: +1 505 663 5335; fax: +1 505 663 5225.
E-mail address: gpark@lanl.gov (G. Park).

actuation, or even self-sensing, within a local area of the structure. One example of documented success using PZT wafers for SHM is impedance-based SHM methods [1].

It is a well-known fact that non-linear dynamic features of a structure are more sensitive to many common types of damage than the linear features. In many cases, damage causes a structure, which exhibits predominantly stationary and linear dynamic response properties in its undamaged state, to exhibit non-stationary and non-linear responses. Common examples of such damage includes cracks or delaminations that open and close when the structure is subjected to normal operating environments and loose parts rattling or sliding against one another. Thus, it is believed that a damage detection scheme that seeks to use non-linear characteristics could enhance the damage classification capability.

In this paper, we experimentally investigated the performance of non-linear features in structure health monitoring. Contrary to most non-linear feature extraction methods, which lie in the low-frequency modal-analysis domain, the features examined in this study are measured at relatively high-frequency ranges with the use of the impedance method. The non-linear features associated with the electro-mechanical impedance measurements are extracted using the frequency domain autoregressive model with exogenous inputs (ARX) model, which explicitly considers non-linear system input/output relationships [2]. The varying sensitivity of the extracted linear and non-linear features in different frequency ranges is also analysed.

The rest of this paper will involve the introduction of the impedance method and the frequency domain ARX model, experiments conducted on a portal frame structure, extraction of linear and non-linear features in various frequency ranges, and qualitative comparison of features.

2. Impedance-based structural health monitoring

The impedance-based health monitoring technique was first proposed by Sun et al. [3] and has since been applied to a wide variety of structures as a promising tool for real-time structural damage assessments [1,4,5–10,11]. The basic concept of this approach is to monitor the variations in structural mechanical impedance caused by the onset of damage. Since structural mechanical impedance measurements are difficult to obtain, impedance methods utilise the electrical impedance of surface bonded piezoelectric materials, which is directly related to the mechanical impedance of the host structure, and will be affected by the onset of structural damage. Through monitoring the measured electrical impedance and comparing it to a baseline measurement, one can qualitatively determine that structural damage has occurred or is imminent. In order to ensure high sensitivity to incipient damage, the electrical impedance is measured at high frequencies (typically greater than 20 kHz). At such high frequencies, the wavelength of the excitation is small and is sensitive enough to detect minor changes in structural integrity. More importantly, high-frequency (kHz) signals require very low voltage (less than 1 V) to produce a useful impedance excitation in the host structure. Another key aspect of the impedance-based methods is the use of PZT materials as a collocated sensor and actuator, in which only one PZT patch can be used for both actuation and sensing of the structural responses. The method has been proved to be effective for detecting various types of damage including corrosion and loose connections. A complete description of the technique can be found in Refs. [1,7].

In SHM, the process of feature extraction is required for the selection of key information from the measured data that distinguishes between a damaged and an undamaged structure. Feature extraction also accomplishes the condensation of a large amount of available data into a much smaller data set that provides concise damage indication. In impedance methods, the damage sensitive features traditionally employed are based on scalar damage metric, such as root mean square deviation (RMSD) or cross-correlation coefficients. In earlier work [3], a simple statistical algorithm, based on frequency-by-frequency comparisons and referred to as "RMSD" has been used,

$$M = \sum_{i=1}^{n} \sqrt{\frac{\left[\text{Re}(Z_{i,1}) - \text{Re}(Z_{i,2})\right]^2}{\left[\text{Re}(Z_{i,1})\right]^2}}, \tag{1}$$

where M represents the damage metric, $Z_{i,1}$ is the impedance of the PZT patch measured at healthy conditions, and $Z_{i,2}$ is the impedance for comparison with the baseline measurement at ith frequency. In an RMSD damage metric chart, the greater numerical value of the metric, the larger the difference between the baseline

and the impedance measurement of interest indicating the presence of damage in a structure. Considering the capacitive nature of PZT materials, the imaginary part has large magnitude as compared to the real part and tends to play a dominant role in the overall magnitude, but has very low sensitivity to damage. Therefore, the real part of the impedance is mainly used for monitoring purpose.

Another scalar damage metric, referred to as the "cross-correlation" metric, can also be used to interpret and quantify information from different data sets. The correlation coefficient between two impedance data sets determines the linear relationship between the two signatures

$$\rho = \frac{1}{n-1} \frac{\sum_{i=1}^{n}(\mathrm{Re}(Z_{i,1}) - \mathrm{Re}(\bar{Z}_1))(\mathrm{Re}(Z_{i,2}) - \mathrm{Re}(\bar{Z}_2))}{\sigma_{Z_1}\sigma_{Z_2}}, \tag{2}$$

where ρ is the correlation coefficient, $Z_{i,1}$ is the baseline FRF data and $Z_{i,2}$ is the FRF data in question at ith frequency, $\bar{Z}_1$ and $\bar{Z}_2$ are the means of the signals and the σ terms are the standard deviations. For convenience, the feature examined is typically $(1-\rho)$ in order to ensure that with increasing damage or change in structural integrity, the metric values also increase. This provides a metric chart that is consistent with other metrics, such as RMSD, in which metric values increase when there is an increase in levels of damage. The cross-correlation metric accounts for vertical and horizontal shifts of impedance signatures, usually associated with temperature changes. In most cases, the results with the correlation metric are consistent with those of RMSD.

The linear features described above are well suited to situations in which one structural state is to be discriminated from another in a linear sense, but they would not be able to quantify any non-linear changes. Because the frequency ranges of impedance measurements are typically high, it is hypothesised that some structural non-linearities will be captured in the measurement. Non-linearity in a structure could manifest itself in an impedance signal in a few different ways. Non-linearities often result in changes in amplitude, peak shifts, and peak shape changes. Non-linearity in a structure can result in changes in the impedance signature with changing input force levels. Non-linearities may also result in frequency response that is correlated to both the input and the output at various frequencies. Therefore, in this paper, we examine the characteristics of a non-linear feature derived from measured impedance signals and its applicability to SHM problems using the frequency domain ARX model, that is detailed in the next section.

3. Frequency domain autoregressive model with exogenous inputs

Frequency response is important in structural dynamics because it relates inputs and outputs of the structure at various frequencies. Analysing these responses can lead to useful information regarding the health of the structure. Conventional frequency response function (FRF) estimators are based on a linearity assumption for the system. Though global behaviours of many large-scale buildings can be approximated in a linear fashion, there are always local non-linearities within the structures. To explicitly consider this non-linearity, a frequency domain ARX inputs is used [2]. In a traditional time-series application, an ARX model attempts to predict response at the current time point based on its own past time point responses, as well as the current and past inputs to the system. A frequency domain ARX model attempts to predict the response at a particular frequency based on the input at that frequency, as well as responses at surrounding frequencies. The responses at the surrounding frequencies are included as inputs to the model to account for subharmonics and superharmonics introduced to the system through non-linear feedback. More details on frequency domain analysis of data using an ARX model can be found in Refs. [2,12].

There are many possible forms of the frequency domain ARX model, with each depending on how the effects of subharmonics and superharmonics are to be considered. In this study, the effects of non-linearities in the system are accounted for by using a first-order model, which is the simplest model available. This first-order ARX model in the frequency domain can be represented as follows:

$$Y(k) = B(k)U(k) + A_1(k)Y(k-1) + A_{-1}(k)Y(k+1), \quad k = 2, 3, \ldots, N_f - 1, \tag{3}$$

where N_f is the highest frequency value examined, $Y(k)$ is the response at kth frequency, $U(k)$ is the input at kth frequency, and $Y(k-1)$ and $Y(k+1)$ are the responses at $(k-1)$th and $(k+1)$th frequencies, respectively.

$A_1(k)$ and $A_{-1}(k)$ are the frequency domain autoregressive coefficients, and $B(k)$ is the exogenous coefficient. While the exogenous coefficient describes the linear effects, the autoregressive coefficients describe any non-linear effects that may be present in the system. If one does not consider the autoregressive coefficients, Eq. (3) becomes traditional FRF estimates. Therefore, in this study, autoregressive coefficients are used to characterise the non-linear nature of damage state, and exogenous coefficients are used for the linear nature of such states.

The unique contribution of this work is that it uses a non-linear feature identification technique in addition to traditional linear features of electrical impedance signals to detect and quantify the damage state of structures. The performance of the non-linear features, especially its enhanced sensitivity (to all types of variability), is compared to that of the linear features.

4. Experimental set-up and procedure

A bolt-jointed, moment-resisting, frame structure was used as a test-bed in this study, shown in Fig. 1. The structure consists of aluminum members connected using steel angle brackets and screws, with a simulated rigid base. Two columns ($6.35 \times 50.8 \times 304.8$ mm) are connected to the top beam ($6.35 \times 50.8 \times 558.8$ mm) using the bolted joints tightened to 17 N m in the healthy condition. PZT patches ($25.4 \times 25.4 \times 0.254$ mm) were mounted on the left side of the symmetric structure (Corner 2), with PZT 1 mounted on the column and PZT 2 mounted on the beam, as shown in Fig. 1.

In order to measure the electrical impedance of the PZT, a simple impedance measuring circuit is used [10]. The voltage into the PZT patch is used as the output to the frequency domain ARX model and the voltage output from the PZT circuit, as seen in Fig. 2, is used as the input. These voltages are measured in the time domain, which is different from the traditional impedance-based methods that only record data in the frequency domain using a sine-sweep test. V_{out} is proportional to the output current of the PZT patch. Electrical impedance of the PZT patch is related to the measured input and output voltage of the PZT wafer
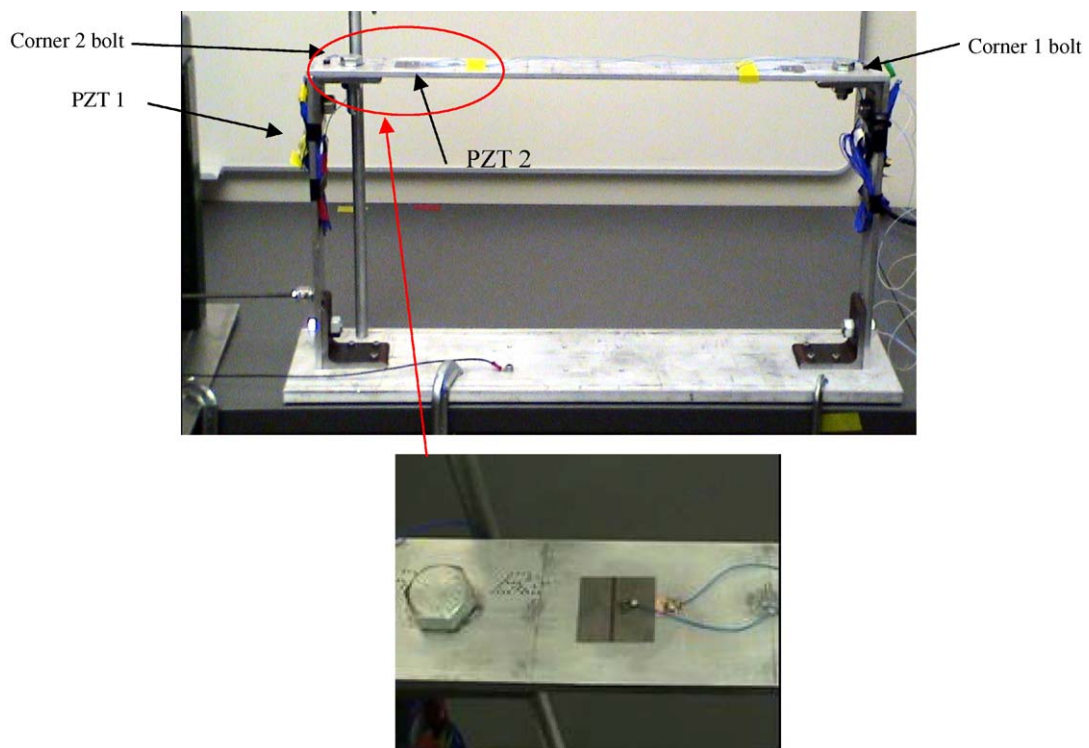

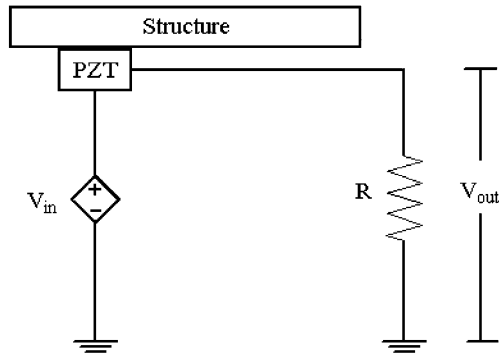Fig. 1. The portal frame structure tested and PZT 2 installed on the top beam.

Fig. 2. Diagram of PZT circuit indicating locations of measured voltages V_{in} and V_{out}.

Table 1
Test matrix for the frame structure

Tests	Structural condition
Baseline	Undamaged
Baseline 1	No change from baseline, measurement after 2 h
Baseline 2	Disassemble/reassemble the top beam
Baseline 3	Disassemble/reassemble the top beam
Baseline 4	No change from baseline 3, measurement after 12 h
Baseline 5	Disassemble/reassemble the top beam
D11	Loosen corner 1 bolt to 8.5 N m
D12	Hand tighten corner 1 bolt
Baseline 6	Retighten to 17 N m
D21	Loosen corner 2 bolt to 8.5 N m
D22	Hand tighten corner 2 bolt

through the following equation:

$$Z_p = \frac{V_p}{I_p} = \frac{V_{in} - V_{out}}{V_{out}/R} \Rightarrow Z_p = R\left(\frac{V_{in}}{V_{out}} - 1\right). \tag{4}$$

A commercial data acquisition system controlled from a laptop PC is used to digitise the voltage analog signals. Time histories were sampled at a rate of 51.2 kHz, producing 32,768 time points. Although the traditional impedance measurements are made at much higher frequency ranges, the current hardware limits our ability to sample in the time domain at frequencies over 51.2 kHz. An amplified random signal (2.5 V) was used as the voltage input for the testing. The value 220 Ω resistor was used to measure the impedance of the PZT patches.

Baseline measurements of a structure should seek to capture all types of variability that the structure might be subject to, which would not be attributed to damage, such as temperature effects. Previous experimentation on this portal frame structure performed by Aumann et al. [13] revealed that variability in the portal frame due to assembly and disassembly is greater than variability introduced by environmental condition changes. Baseline measurements in this set of experiments attempts to capture, to some extent, typical environmental variability and assembly/disassembly variability by disassembling the top beam in order to establish a true decision limit for damage indications. Therefore, a total of 6 baseline time histories were recorded for both PZT patches, with conditions noted in Table 1. Four damage states were then introduced at two different locations by loosening the bolts at those locations to 8.5 N m and then to hand tight. After implementing the

damage, the time histories were again recorded from each PZT. The full test matrix, which was performed sequentially, is shown in Table 1.

All time history data are first standardised by subtracting the mean and dividing by the standard deviation, as in the following Eq. (5):

$$\bar{x} = \frac{x - \mu}{\sigma}, \tag{5}$$

where **x** is the original vector, $\bar{x}$ the normalised vector, μ the mean of the original vector, and σ the standard deviation of the original vector. This process is used so that the damage detection algorithm can distinguish between structural damage and operational variability [14]. Because $Y(k)$ and $U(k)$ in Eq. (3) are complex numbers, the coefficients $B(k)$, $A_1(k)$ and $A_{-1}(k)$ coefficients are also complex. Therefore, for each frequency k, there are 6 unknown coefficients that must be determined. In order to estimate the ARX coefficients, multiple sets of data need to be recorded while the structure is in the same condition. Because only one 32,768-point time history is available for each condition, each time history is split up into 29 separate 4096-point blocks with 75% overlap. A Hanning window is applied to each block of data. A fast Fourier transform (FFT) is then performed on all data blocks in order to transfer the time history information into the frequency domain. There are 29 equations (from the 29 FFTs) and 6 unknown coefficients, for each frequency value k, that must be solved. $\mathbf{B}(k)$, $\mathbf{A}_1(k)$ and $\mathbf{A}_{-1}(k)$ in Eq. (4) are then determined by minimising the sum of the squared error associated with how well the ARX model in Eq. (4) describes the measured impedance data.

5. Analysis of linear and non-linear features from impedance data

Quantification of the differences between the baselines and the damage cases through application of linear and non-linear feature extraction methods is the subject of this section. While the structure exhibits global linearity, it was hypothesised that non-linearities would be present in the data due to the contacting interfaces of the parts and differences in these interfaces introduced in assembly/disassembly of the top beam. Cross-correlation coefficients are calculated and used to assess the conditions of the structure. Cross correlations of linear and non-linear coefficients were calculated between six baseline measurements and each tested case. The first baseline is used as a "true" undamaged signature, to which all other measurement are compared.

5.1. Linear feature

The real parts of the linear coefficients for PZT 1 and PZT 2 are plotted in Fig. 3(a) and (b), respectively, in the frequency range of 10–20 kHz. It should be noted that, in the impedance methods, only the real part is
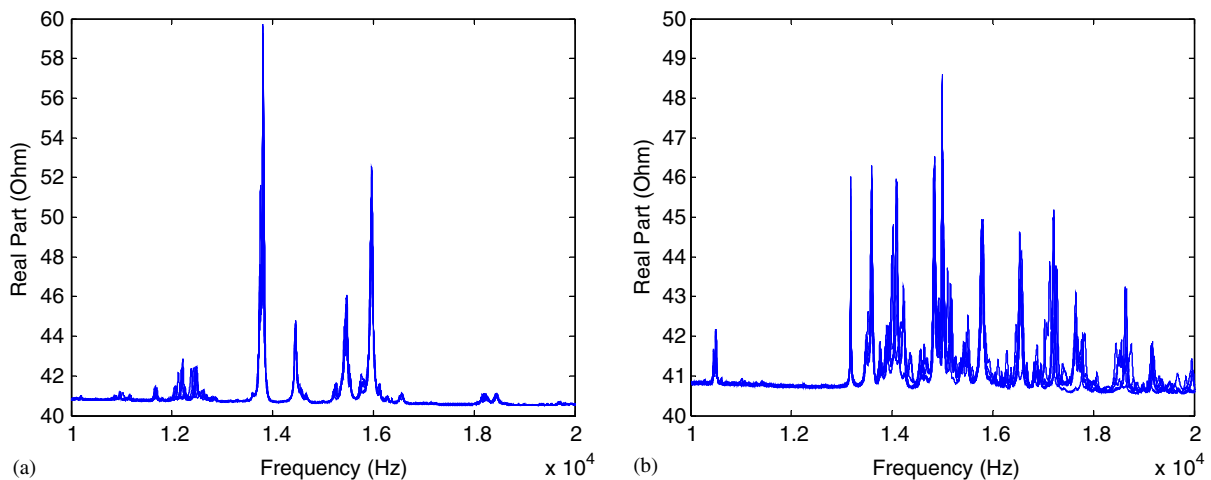

Fig. 3. Baselines of linear coefficients. Six measurements are shown without label. A relatively large variation was observed in PZT 2: (a) PZT 1; (b) PZT 2.

usually used for monitoring structures because it is more sensitive to structural damage than the imaginary part [1]. Therefore, for the frequency ARX model, only the real part is used for the analysis. For PZT 1, even after the assembly/disassembly procedure, the impedance signatures are repeatable and show relatively small changes. The variation is anticipated to increase in PZT 2 because PZT 2 is installed on the top-beam (the component that is disassembled and reassembled). Large baseline variations in PZT 2 can be observed. The variation in the signal due to damage needs to be greater than the baseline variations in order to be detectable.

Fig. 4 illustrates PZT 2's baselines and signals that were measured after the damage at Corner 2 (D21, D22 in Table 1). It is easy to see that qualitatively that damaged signals are quite different with the appearance of new peaks and shifts, especially at the higher frequency levels. With increasing levels of the damage, the impedance variation also becomes more noticeable. The other results, i.e. PZT 1 for D21, D22 and PZT 2 for D11, D12, are similar. The size of the structure and relatively low impedance frequency range (10–20 kHz) employed limits the ability of the PZT patches to detect damage "locally". Both PZT patches show some sensitivity to damage at Corner 1 and Corner 2. The impedance frequency must be kept higher in order for the damage to be localised, because then the PZT patches are sensitive to the damage in the near field and less sensitive to changes in far field.
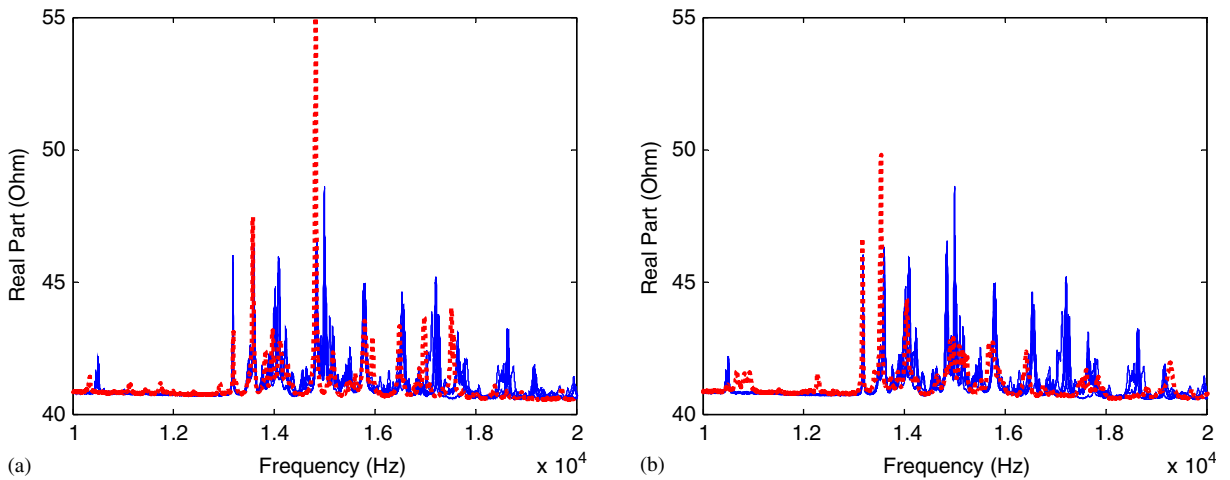

Fig. 4. PZT 2, Linear coefficients of baselines and damage at corner 2: (a) Baselines and D21 (8.5 N m); (b) baselines and D22 (hand tightened).
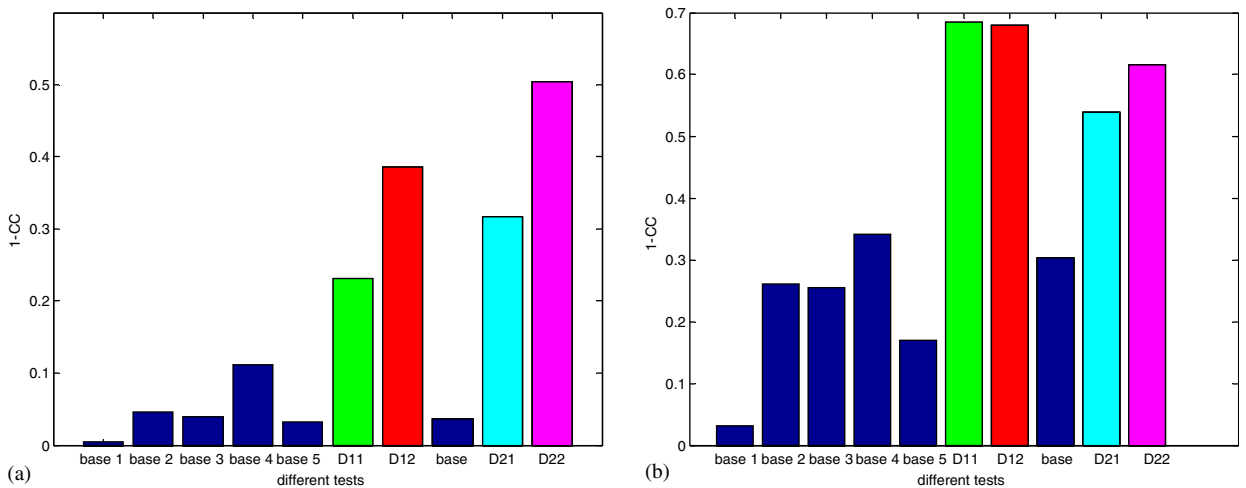

Fig. 5. Cross correlation damage metric chart of linear feature at 10–20 kHz: (a) PZT 1; (b) PZT 2.

Quantification of damage was the next step. Results for PZT 1 and PZT 2 are shown in Figs. 5. Cross correlations confirm what was suspected upon initial observation of the signals. The frequency employed and size of the structure limits the ability of the PZT patches to detect damage locally at Corner 1. However, the cross correlation of PZT 1 reveals that it may distinguish between the 8.5 N m case and the hand tightened damage cases. The extent and distance of damage is somewhat related to the coefficients values. The cross correlation of PZT 2 does not show the same characteristics. It shows relatively large variations compared to PZT1 and it is only able to distinguish between damaged and undamaged states of the portal frame. This could be because of the close proximity of PZT2 to both of the damaged joints and its location on the top beam that is being assembled and disassembled. It should be noted that the linear coefficients and their changes with induced damage follow essentially the same pattern of the traditional impedance signals, which were measured by the impedance analyser.

5.2. Non-linear feature

Fig. 6 show the baselines superimposed with the damage case (D22) for non-linear coefficients of both PZT patches, in the frequency range of 12–17 kHz. From the figures, it is apparent that the damaged non-linear signatures differ from the undamaged cases significantly. In order to quantify this difference, a cross correlation was calculated for the non-linear coefficients. Analysis of the non-linear coefficients yielded some interesting results, as shown in Fig. 7. The variations of baselines are relatively large compared to those of the linear coefficients. Because of relatively larger variations, the first damage (D11) could not be definitely identified by PZT 1. On the other hand, the non-linear coefficients of PZT 1 are somewhat over-sensitive to the presence of other damage cases (D12, D21, D22). For PZT 2, because of the direct contact with the top beam and the damaged joint, baseline variations are much larger and damaged cases are not definitely identified.

It can be concluded from the figures that the non-linear coefficients might be too sensitive at higher frequency ranges. The linear coefficients, which are shown in Figs. 4 and 5, seem to provide a better characterisation regarding the conditions of the structure. While non-linear system identification methods proved to have a better sensitivity for damage detection at lower, modal frequency ranges, its applicability at higher frequency ranges should be carefully considered because of "over-sensitivity" to all types of variability, as shown in this example.

The next step of this investigation is to examine the sensitivity of non-linear coefficients at different frequency ranges. For this purpose, FRFs between PZT 1 and PZT 2, instead of electrical impedances, were used. This is because the low-frequency ranges of electrical impedance are dominated by the capacitive nature of the piezoelectric materials, which imposes the difficulties in accurately assessing the characteristics of low-frequency data. The impedance data is then analysed after we identify the sensitivities of the coefficients from
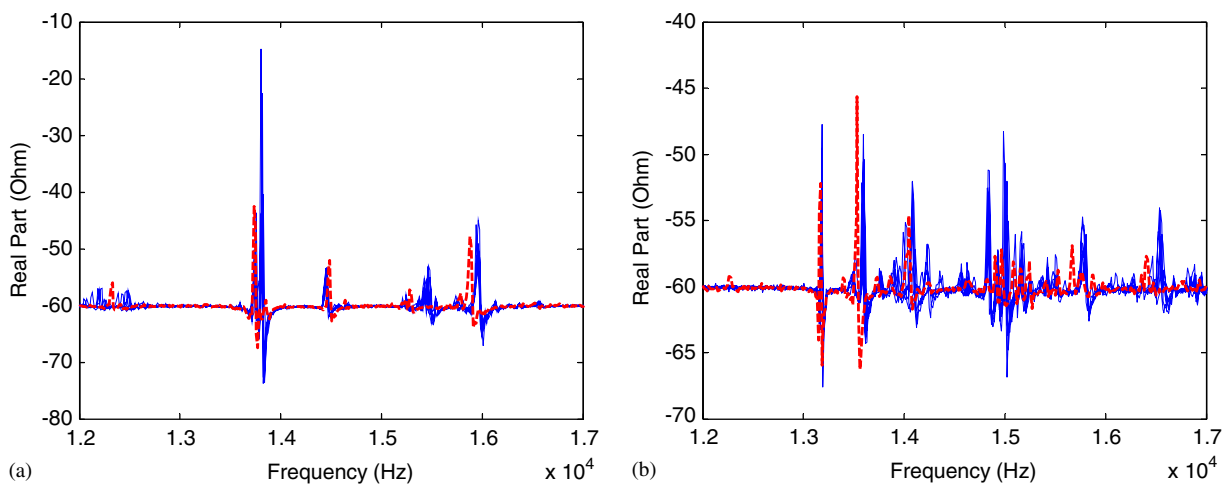

Fig. 6. Nonlinear coefficients, baselines and D22: (a) PZT 1; (b) PZT 2.

the FRF measurements. The same experimental and analytical procedures are used as with the impedance method. As confirmed in the previous studies [1,15], the imaginary part of FRF is analogous to the real part of the electrical impedance (linear coefficients). Therefore, only the imaginary parts of FRF are examined, to be consistent with the impedance analysis. Fig. 8 shows the imaginary part of the linear coefficients of the FRF between PZT1 and PZT2 with induced damage (D12).

The correlations were examined for linear and non-linear coefficients at two different frequency bands, 0–2 kHz and 15–23 kHz as shown in Figs. 9 and 10. At lower frequency ranges, the linear coefficients could not definitively identify the small-scale damage cases (torque reduced to 8.5 N m), but the non-linear coefficients could. In this case, the non-linear features increased sensitivity makes it superior to the linear features at lower frequency ranges, as confirmed by numerous studies [12,16]. At higher frequency ranges, however, the non-linear feature seems to be somewhat over-sensitive to baseline variations, and presence of damage is not as clear. On the other hand, the linear feature has much more baseline repeatability and improved sensitivity, and hence it can discriminate between baselines and all damage cases. These observations from FRF data confirm
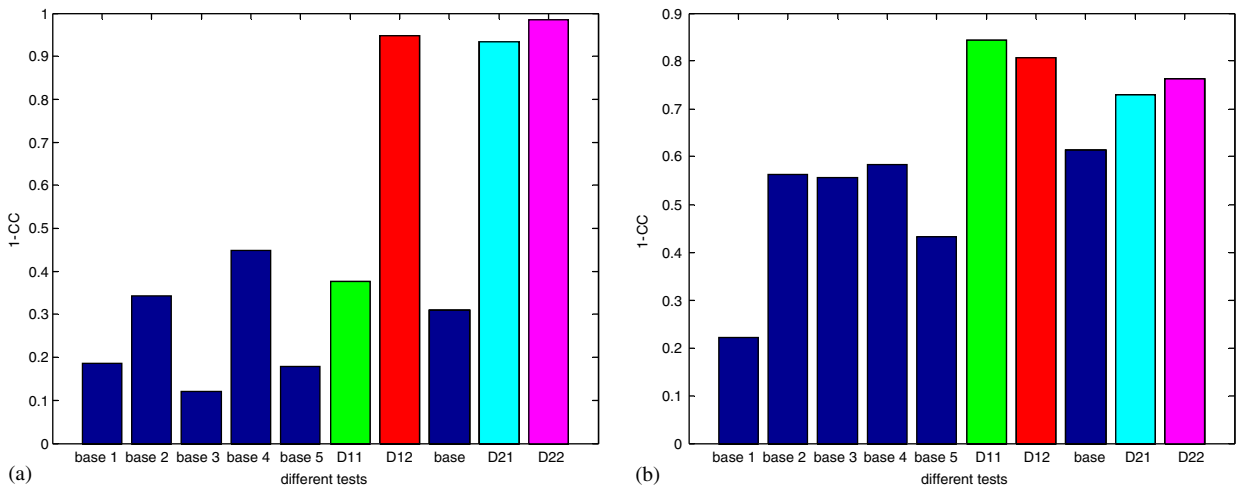

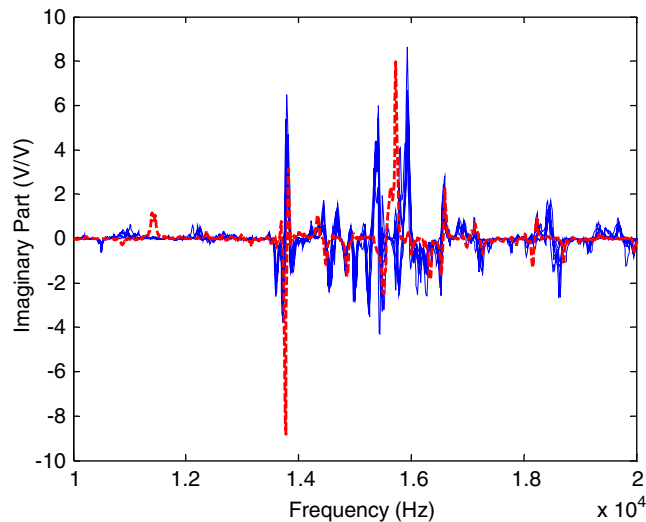Fig. 7. Correlation of non-linear coefficient, 10-20 kHz: (a) PZT 1; (b) PZT 2.

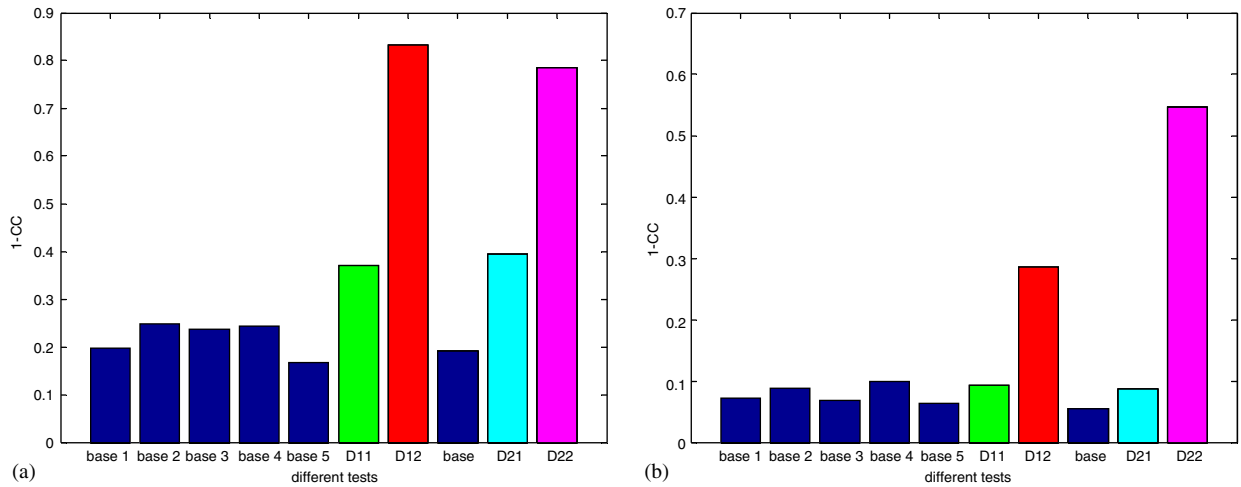Fig. 8. Linear coefficients from FRF between PZT1, baselines and D12.

Fig. 9. Correlation of non-linear and linear coefficients, PZT 1-2 FRF, 0-2 kHz: (a) non-linear coefficient; (b) linear coefficient.
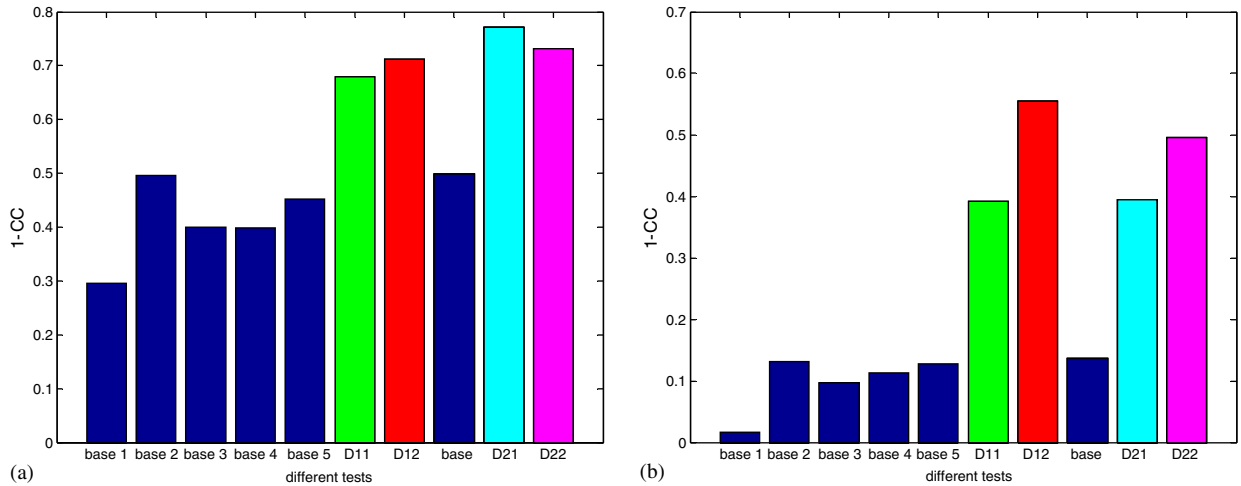

Fig. 10. Correlation of non-linear and linear coefficients, PZT 1-2 FRF, 15-23 kHz: (a) non-linear coefficient; (b) linear coefficient.

what has been observed in the previous studies combining non-linear features and impedance sensing. Based on these results, the non-linear coefficients of the impedance data were once again analysed, but this time in just the lower frequency ranges at 1–4 kHz. All damage cases could be successfully identified as shown in Fig. 11.

6. Discussion

It can be concluded from these observations that non-linear features, in the form of non-linear ARX model coefficients, demonstrated varying sensitivity to damage depending on the frequency range examined with increased sensitivity (to all types of variability) at higher frequency ranges. Some other non-linear features, including reciprocity checks, changes in the magnitude of applied force (FRF distortions), and time-domain AR-ARX models, show the same kind of characteristics.

This quality of non-linear features could be leveraged in several ways, however. First, signal processing techniques that capitalise on the increased sensitivity could be utilised. In this study, we only examined
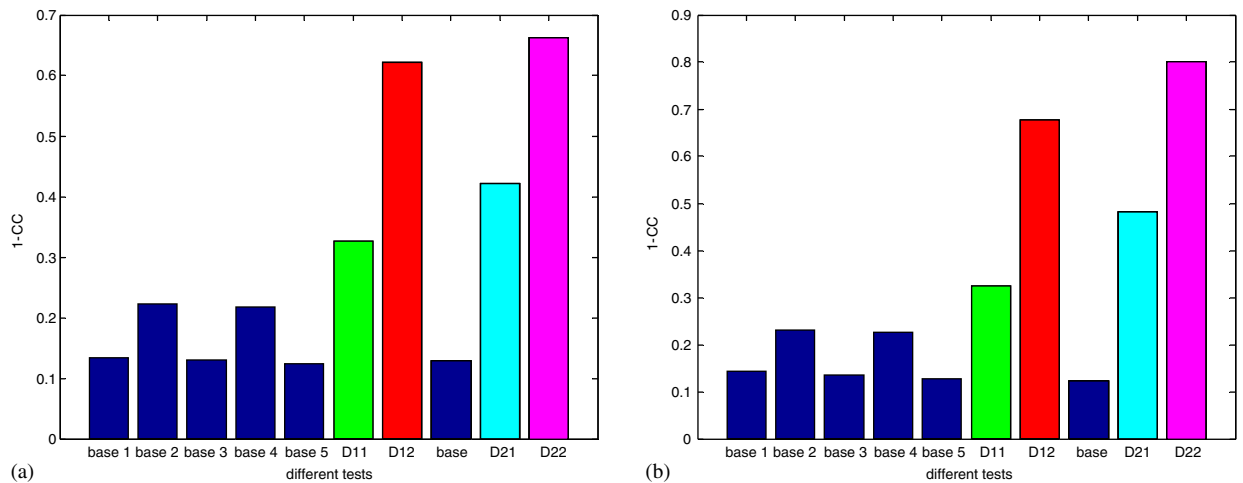
Fig. 11. Correlation of non-linear coefficients, PZT 1, 1-4 kHz: (a) PZT 1; (b) PZT 2.

cross-correlation coefficients to assess the performance of the non-linear feature (and the RMSD shows similar results). Other statistical feature extraction methods could be used in concert with the ARX non-linear coefficients (such as moments, variance normalised coefficients, etc.) to utilise the improved sensitivity to damage and potentially decreasing baseline variability. Another desirable quality of the low-frequency range sensitivity of the non-linear coefficients is that hardware sampling and data storage requirements could be relaxed. The changing sensitivity of non-linear features with frequency range could be leveraged for sensor locations that are not ideal; i.e., sensors that are far field from damage could have increased sensitivity by looking at non-linear coefficients for the higher frequency ranges. Finally, Because of the similarity between the linear coefficients and the original impedance signals, the non-linear feature, especially in the form of the frequency domain ARX model, could be used as supplementary information for the linear features. This approach could result in confirmatory and somewhat redundant information for better performance in SHM.

7. Conclusions

Both linear and non-linear features of piezoelectric impedance are analysed for SHM applications. A series of experiments was performed on a portal frame. The linear feature shows an excellent capability at higher frequency ranges. Non-linear features, in the form of non-linear ARX model coefficients, demonstrated varying sensitivity to damage depending on the frequency range examined, with increased sensitivity (to all types of variability) at higher frequency ranges. This work further reinforces the utility of the use of non-linear features for damage identification. Future work will include more investigation into binning of frequency ranges when using ARX coefficients, changing window size when fitting ARX models, looking at additional statistical feature extraction methods, and testing of more complex structures.

Acknowledgements

References

[1] G. Park, H. Sohn, C.R. Farrar, D.J. Inman, Overview of piezoelectric impedance-based health monitoring and path forward, The Shock and Vibration Digest 35 (6) (2003) 451–463.
[2] D.E. Adams, Frequency domain ARX models and multi-harmonic FRF estimators for nonlinear dynamic systems, Journal of Sound and Vibration 250 (5) (2001) 935–950.

[3] F.P. Sun, Z. Chaudhry, C. Liang, C.A. Rogers, Truss structure integrity identification using PZT sensor-actuator, Journal of Intelligent Material Systems and Structures 6 (1995) 134–139.

[4] V. Giurgiutiu, A.N. Zagrai, J.J. Bao, J.M. Redmond, D. Roach, K. Rackow, Active Sensors for health monitoring of aging aerospace structures, International Journal of Condition Monitoring and Diagnostic Engineering Management 6 (1) (2003) 3–21.

[5] G. Mook, J. Pohl, M. Michel, Non-destructive characterization of smart CFRP structures, Smart Materials and Structures 12 (2003) 997–1004.

[6] K.K. Tseng, M.L. Tinker, J.O. Lassiter, D.M. Peairs, Temperature dependency of impedance-based nondestructive testing, Experimental Techniques 27 (5) (2003) 33–36.

[7] S. Bhalla, C.K. Soh, Structural impedance-based damage diagnosis by piezo-transducers, Earthquake Engineering and Structural Dynamics 32 (12) (2003) 1897–1916.

[8] S. Bhalla, C.K. Soh, High frequency piezoelectric signatures for diagnosis of seismic/blast induced structural damages, NDT&E International 37 (1) (2004) 23–33.

[9] C. Bois, C. Hochard, Monitoring of laminated composites delamination based on electro-mechanical impedance measurement, Journal of Intelligent Material Systems and Structures 15 (1) (2004) 59–67.

[10] D. Peairs, G. Park, D.J. Inman, Improving accessibility of the impedance-based structural health monitoring method, Journal of Intelligent Material Systems and Structures 15 (2) (2004) 129–140.

[11] M. Abe, Y. Fujino, T. Miyashita, Quantitative health monitoring of bolted joints using a piezoceramic actuator-sensor, Smart Materials and Structures 13 (1) (2004) 20–29.

[12] D.E. Adams, C.R. Farrar, Identifying linear and nonlinear damage using frequency domain ARX models, International Journal of Structural Health Monitoring 1 (2) (2002) 185–201.

[13] R.J. Aumann, A.S. McCarty, C.C. Olson, Identification of random variation in structures and their parameter estimates. Proceedings of the 22nd International Modal Analysis Conference, Society of Experimental Mechanics, Kissimmee, FL, 2003.

[14] H. Sohn, J.J. Czarnecki, C.R. Farrar, Structural health monitoring using statistical process control, ASCE Journal of Structural Engineering 126 (11) (2000) 1356–1363.

[15] V. Giurgiutiu, A.N. Zagrai, Embedded self-sensing piezoelectric active sensors for online structural identification, ASME Journal of Vibration and Acoustics 124 (1) (2002) 116–125.

[16] S.W. Doebling, C.R. Farrar, M.B. Prime, A summary review of vibration-based damage identification methods, The Shock and Vibration Digest Journal 30 (1998) 91–105.